JOURNAL OF THEORETICAL AND APPLIED MECHANICS
63, 1, pp. 13-26, Warsaw 2025
https://doi.org/10.15632/jtam-pl/194501

INVESTIGATION ON IMPACT PROTECTION EFFECTIVENESS OF CUSHIONING MATERIAL IN PACKAGING CONTAINER UNDER LATERAL CONSTRAINT CONDITION

Zexiong Zhang

University of Science and Technology of China, Department of Modern Mechanics, Hefei, Anhui, China, and Shock and Vibration of Engineering Materials and Structures Key Laboratory of Sichuan Province, Mianyang, China
e-mail: jz1108@mail.ustc.edu.cn (Zexiong Zhang); lijiaxing21@gscaep.ac.cn (Jiaxing Li)

Weizhou Zhong, Jiaxing Li

Shock and Vibration of Engineering Materials and Structures Key Laboratory of Sichuan Province, Mianyang, China
corresponding author Weizhou Zhong, e-mail: zhongwzcaep@126.com

Jingrun Luo

University of Science and Technology of China, Department of Modern Mechanics, Hefei, Anhui, China, and Shock and Vibration of Engineering Materials and Structures Key Laboratory of Sichuan Province, Mianyang, China
e-mail: luojr@caep.cn

A theoretical model is proposed to evaluate the impact protection effectiveness of a porous cushioning material in a packaging container under the lateral constraint condition. An acceleration-displacement equation of the protected product in the packaging container is derived. The reliability of the equation is validated by numerical simulation. Subsequently, the equation is applied to analyse the effect of strain rate on impact protection effectiveness of three polymer foams under the lateral constraint condition, and to design the thicknesses of cushioning materials in the packaging container.

Keywords: impact protection, packaging container, cushioning material, lateral constraint, numerical simulation

1. Introduction

The impact-resistant packaging container generally consists of the outer shell, cushioning material and protected product. The cushioning material is usually filled between the protected product and the outer shell. The mechanical behaviour of the cushioning material determines the impact protection effectiveness of the packaging container. Therefore, evaluating the energy absorption of the cushioning material and optimizing cushioning material configuration are feasible approaches to improve the protective performance of the packaging container.

The mechanical behaviour and energy dissipation of the cushioning material greatly affect the protection effectiveness of the packaging container. Many scholars focus on promoting the energy absorption of cushion materials in recent years. For pre-designing configuration of cushioning materials, Meng *et al.* (2020) examined the mechanical response of composite materials made of honeycomb aluminium under explosive impact loads, and proposed an empirical formula to characterize the compression depth of double-layer honeycomb aluminium composite materials. Kader *et al.* (2016) assessed the shock propagation and elastic-plastic deformation behaviour of a closed-cell aluminium foam by experiments and numerical simulations. The results showed the significant influence of the foam material topology on the shortest path for stress wave propagation in a porous material. Estrada *et al.* (2017) analysed the sizing effect of discontinuities on energy absorption characteristics of a steel square

profile. It indicated that pre-designed discontinuities effectively enhanced energy absorption in square-section steel tubes, whereas reduced the peak load. Baroutaji *et al.* (2016) analysed the energy absorption characteristics of nested circular tube structures under lateral loads, and explored the effects of geometrical and loading parameters on the responses of the best nested tube system. Sek and Rouillard (2006) investigated the response characteristics of multi-layer corrugated cardboard cushioning systems under impact loads, and demonstrated that adding anti-wrinkle liners to soft cardboard cushion pads significantly expanded their protective coverage and capability to withstand extreme conditions. Guo *et al.* (2021) investigated the mechanical behaviour and cushioning energy absorption of paper composite sandwich structures with sinusoidal corrugation and hexagonal honeycomb cores. They showed that the influence of static compression rate on the yield strength and cushioning energy absorption of the paper composite sandwich structure was not obvious, and the composite sandwich structures with large inertia moment and large thickness had more excellent cushioning energy absorption.

Moreover, cushion materials with gradient density can be designed to improve energy absorption. Baertsch *et al.* (2021) optimized an auxetic re-entrant structure with a stiffness gradient for enhanced energy absorption with a low acceleration peak, and found that concave honeycomb structures with gradient stiffness variations exhibited superior energy absorption capability. Zeng *et al.* (2010) investigated the influence of the density gradient profile on the mechanical response of graded polymeric hollow sphere agglomerates under an impact loading. They showed that foam materials with gradient density or stiffness had a stronger cushioning effectiveness along the direction of gradient variation. Koohbor and Kidane (2016) proposed a semi-analytical approach to study the effect of density gradation in graded polymeric foams. A strong concave gradient was shown to promote substantially lighter structural weights with superior energy absorption. Gputa (2007) found that the compressive modulus, strength, and total energy absorption of syntactic foams could be controlled by an appropriate type and volume fraction of microballoons. The compressive strength and modulus of a functionally graded syntactic foam were dependent on the weakest layer in their structure. The literature indicates that optimization of structure topology and gradient configuration is a feasible approach to enhance the energy absorption of the cushioning material.

Apart from the studies on mechanical behaviour and energy dissipation of cushioning materials, many scholars (Lye *et al.*, 2004; Chang *et al.*, 2017; Zhang *et al.*, 2011; Pan and Yu, 2022) have performed impacting experiments to evaluate the impact protection effectiveness of packaging container systems. Luong *et al.* (2021) analysed the effects of repeated impacts on corrugated paper packaging by numerical simulations and experimental tests. An elastoplastic homogenization model was proposed to replace a corrugated-core sandwich panel by a homogeneous plate. Hussain *et al.* (2021) investigated the energy absorption of composite material automotive crash boxes using drop-weight impact tests. The strength-to-weight ratio was considered as the important factor for the packaging boxes made of different cross-sections cushion materials. An and Shi (2022) proposed an innovative reliability optimization method for cushioning design based on the dynamic stress-strain curve and an active set strategy. It provides a new design method for cushioning packaging based on the dynamic cushioning material stress-strain curve. In the aforementioned literatures, the cushioning materials are usually taken as fully compressible materials, ignoring the influence of lateral constraint conditions. A porous material volume exhibits incompressible characteristics in the compaction stage. The lateral constraint makes the cushion material stress increasing greatly with strain in the compaction process. It is necessary to investigate the compressive behaviour of cushioning materials under lateral constraint conditions, which contributes to improve the cushion evaluation and the optimization design of the packaging container.

For a packaging container with a high strength outer shell, the cross-sectional area of the porous cushioning material can be taken as constant during the impact compression process. Based on the stress wave theory and propagation characteristics of stress waves in a porous material (Reid and Peng, 1997; Karagiozova, 2011), the acceleration of the protected product can be derived to evaluate the cushioning protection effectiveness of the packaging container. The theoretical model of the drop impact for cushioning material packaging containers is established, and the acceleration-displacement equation for the protected product is given in the paper. The equation indicates the peak acceleration of the protected product, which is influenced by density, platform stress and compaction strain of the cushioning material. Combining the mechanical properties of an expanded polystyrene foam (EPS), flexible polyurethane foam (FPUF) (Zhang *et al.*, 2023), and rigid polyurethane foam (RPUF) (Zhang *et al.*, 2022), the theoretical equation is verified by numerical simulations. The influence of the strain rate on the impact protection effectiveness of the three polymer foam materials under the lateral constraint condition is analysed, then the equation for computing the optimal thickness of the cushioning material in the packaging container is derived.

2. Theoretical model of the packaging container drop impact

2.1. Fundamental equation for the stress wave in a porous cushioning material

The stress-strain curve of porous materials exhibits a concave characteristic in the plastic stage. When a high amplitude stress wave propagates in a porous material, the material undergoes compaction and "shock waves" are generated. Ignoring the stress reflection or "shock waves" interaction, the stress in the porous material can be simplified in Eq. (2.1) (Karagiozova, 2011)

$$\sigma(\varepsilon) = \begin{cases} \sigma_p & 0 \leqslant \varepsilon < \varepsilon_D \\ +\infty & \varepsilon_D \leqslant \varepsilon \end{cases} \tag{2.1}$$

where σ, ε is stress and strain, σ_p is plastic platform stress and ε_D is compaction strain.

Figure 1 shows a schematic of a strong discontinuity wave front. The physical variables S^+ and S^- show the states in ahead and behind wave front, respectively. The difference between the value is denoted as $[S]$. The C, A, v and x are wave propagation velocity, section area, velocity and displacement, respectively.

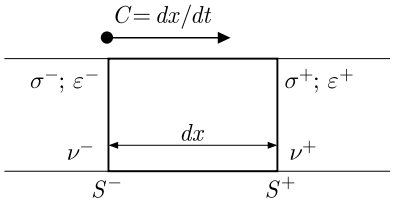

Fig. 1. Schematic of strong intermittent wave front propagation

The momentum conservation condition of the wave front is as follows

$$(\sigma^+ - \sigma^-)Adt = \rho AdX(v^- - v^+) \qquad [\sigma] = -\rho C[v] \tag{2.2}$$

The displacement continuity condition is expressed as

$$\frac{d}{dt}[u] = [X_{,t}] + C[X_{,x}] = [v] + C[\varepsilon] = 0 \qquad [v] = -C[\varepsilon] \tag{2.3}$$

The energy conservation equation is given below, where e is the internal energy per unit mass of the porous material

$$
\begin{aligned}
&(\sigma^+ v^+ - \sigma^- v^-)Adt = (e^- - e^+)\rho A dX + \frac{1}{2}\rho A dX\{(v^-)^2 - (v^+)^2\} \\
&[\sigma v] = -\rho C[e] - \frac{1}{2}C\rho[v^2] \\
&-\rho C[e] = [\sigma v] + \frac{1}{2}C\rho[v^2] = [\sigma v] + \frac{1}{2}C\rho[v](v^+ + v^-) = [\sigma v] - \frac{1}{2}[\sigma](v^+ + v^-) \\
&-\rho C[e] = \sigma^+ v^+ - \sigma^- v^- - \frac{1}{2}(\sigma^+ v^+ + \sigma^+ v^- - \sigma^- v^+ - \sigma^- v^-) \\
&-\rho C[e] = \frac{1}{2}(\sigma^+ + \sigma^-)(v^+ - v^-) \\
&\rho C[e] = -\frac{1}{2}(\sigma^+ + \sigma^-)[v] = \frac{1}{2}(\sigma^+ + \sigma^-)C[\varepsilon] \\
&\rho[e] = \frac{1}{2}(\sigma^+ + \sigma^-)[\varepsilon]
\end{aligned}
\tag{2.4}
$$

2.2. Acceleration-displacement equation for the protected product

During impacting the packaging container, the cushioning material is usually constrained by the outer shell. The cross-section area of the cushion layer can be taken as constant. In order to analyse theoretically analyse the acceleration response of the protected product during impact process, the packaging container is simplified as shown in Fig. 2. It only consists of the protected product, cushioning material and target. The left subfigure shows the undeformed state of the packaging container at the initial moment. The middle subfigure represents the deformation state of the packaging container at a certain moment t. The right subfigure represents the deformation state of the packaging structure at a certain moment $t + \Delta t$. M_a, ρ_0 and A are mass, density and section area of the cushioning material in the original stage, respectively. σ_d and ρ_D are stress and density of the cushioning material in the densification stage, respectively. M_b is mass of the protected product and C is the stress wave propagation speed in the cushion material. It is assumed that the cushion material is compressed into the densification layer in the impact process. The white and blue areas denote the uncompacted part and the densification part of the cushion material, respectively.

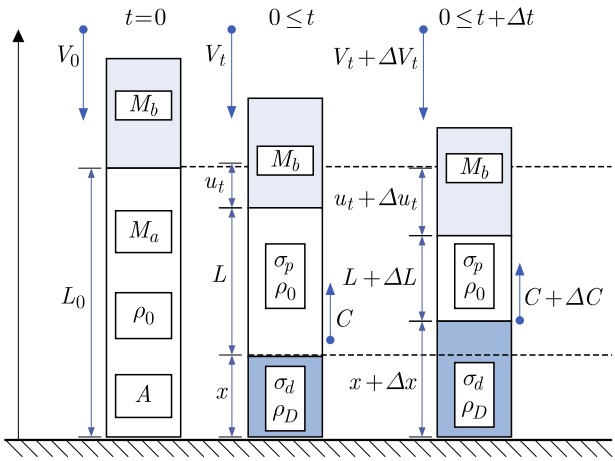

Fig. 2. Drop model of the packaging container

The variables ahead the wave front are as follows

$$
v^+ = V_t \qquad \varepsilon^+ = 0 \qquad \sigma^+ = \sigma_p \qquad \rho^+ = \rho_0 \tag{2.5}
$$

The variables behind the wave front are

$$v^- = 0 \qquad \varepsilon^- = \varepsilon_D \qquad \sigma^- = \sigma_d \qquad \rho^- = \rho_D = \frac{\rho_0}{1-\varepsilon_D} \tag{2.6}$$

where σ_d represents the dynamic stress. Based on Eqs. (2.2), (2.3), (2.5) and (2.6), the equations $[\sigma] = -\rho C[v]$ and $V_t = -C[\varepsilon]$ can be expressed as

$$\sigma_p - \sigma_d = -\rho_0 C(V_t - 0) = -\frac{\rho_0 V_t^2}{\varepsilon_D} \qquad \sigma_d = \sigma_p + \frac{\rho_0 V_t^2}{\varepsilon_D} \tag{2.7}$$

The length of the undeformed zone is as follows

$$L = L_0 - u_t - x \tag{2.8}$$

In Fig. 2, the porous cushioning material with initial length $u_t + x$ is compressed into the densification layer with length x. The strain ε_D can be defined as the ratio of the reduced length to the original length

$$\begin{aligned} &\varepsilon_D = \frac{u_t}{u_t + x} \qquad x = \frac{1-\varepsilon_D}{\varepsilon_D} u_t \\ &u_t + x = u_t + \frac{1-\varepsilon_D}{\varepsilon_D} u_t = \frac{u_t}{\varepsilon_D} \end{aligned} \tag{2.9}$$

According to Eq. (2.8) and Eq. $(2.9)_3$, the following equation can be given

$$\frac{dL}{dt} = -\frac{d(u_t + x)}{dt} = -\frac{1}{\varepsilon_D}\frac{du_t}{dt} = -\frac{V_t}{\varepsilon_D} \tag{2.10}$$

Based on displacement continuity and conservation of momentum and energy, the internal energy of the packaging container is constant. The compression of the porous cushioning material results in a change of internal energy ΔE_U. If the reduced length is ΔL, the internal energy variation is as follows

$$\begin{aligned} \Delta E_U &= E_{U2} - E_{U1} = \rho[e]A\Delta L = \frac{1}{2}(\sigma_d + \sigma_p)[\varepsilon]A\Delta L = \frac{1}{2}\Big(2\sigma_p + \rho_0\frac{V_t^2}{\varepsilon_D}\Big)(0-\varepsilon_D)A\Delta L \\ &= -\Big(\sigma_p + \frac{\rho_0 V_t^2}{2\varepsilon_D}\Big)\varepsilon_D A\Delta L \end{aligned} \tag{2.11}$$

The compaction part of the cushioning material has velocity 0, while the velocity of the protected product and the uncompressed part of the cushioning material is V_t. The change in kinetic energy ΔE_K of the packaging container can be obtained by following equations

$$\begin{aligned} \Delta E_K &= E_{K2} - E_{K1} = \frac{1}{2}\{M_b + \rho_0(L+\Delta L)A\}(V_t + \Delta V_t)^2 - \frac{1}{2}(M_b + \rho_0 LA)V_t^2 \\ &= \frac{1}{2}M_b(\Delta V_t^2 + 2V_t\Delta V_t) + \frac{1}{2}\rho_0 LA(\Delta V_t^2 + 2V_t\Delta V_t) + \frac{1}{2}\rho_0\Delta LA(V_t + \Delta V_t)^2 \\ &= M_b V_t\Delta V_t + \rho_0 LAV_t\Delta V_t + \frac{1}{2}\rho_0\Delta LAV_t^2 + O\{(\Delta V_t^2 + 2\Delta L\Delta V_t + \Delta L\Delta V_t^2\} \end{aligned} \tag{2.12}$$

Ignoring higher order infinitesimals, the formula is simplified to

$$\Delta E_K = M_b V_t\Delta V_t + \rho_0 LAV_t\Delta V_t + \frac{1}{2}\rho_0\Delta LAV_t^2 = \frac{1}{2}\{2V_t(M_b + \rho_0 LA)\Delta V_t + \rho_0 V_t^2\Delta L\} \tag{2.13}$$

The total energy change of the packaging container is zero, as in the following

$$\Delta E_U + \Delta E_K = 0 \qquad \Delta E_K = -\Delta E_U \tag{2.14}$$

The packaging container energy conservation equation is expressed as

$$M_b V_t \Delta V_t + \rho_0 L A V_t \Delta V_t + \frac{1}{2}\rho_0 \Delta L A V_t^2 = \Big(\sigma_p + \frac{\rho_0 V_t^2}{2\varepsilon_D}\Big)\varepsilon_D A \Delta L \tag{2.15}$$

Then, Eq. (2.8) and Eq. $(2.9)_1$ can be written as

$$\begin{aligned} &M_b V_t \Delta V_t + \rho_0 (L_0 - u_t - x) A V_t \Delta V_t + \frac{1}{2}\rho_0 \Delta L A V_t^2 = \sigma_p \varepsilon_D A \Delta L + \frac{1}{2}\rho_0 V_t^2 A \Delta L \\ &M_b V_t \Delta V_t + \rho_0 \Big(L_0 - \frac{u_t}{\varepsilon_D}\Big) A V_t \Delta V_t = \sigma_p \varepsilon_D A \Delta L \end{aligned} \tag{2.16}$$

Equation $(2.16)_2$ is divided by dt and the limit of dt is close to 0. The acceleration-displacement equation of the protected product is obtained

$$\Big(M_b V_t + \rho_0 L_0 A V_t - \frac{\rho_0 A}{\varepsilon_D} u_t V_t\Big)\frac{dV_t}{dt} = \sigma_p \varepsilon_D A \frac{dL}{dt} \tag{2.17}$$

According Eq. (2.10) and Eq. (2.17), the following equation can be obtained

$$\begin{aligned} &\Big(M_b V_t + \rho_0 L_0 A V_t - \frac{\rho_0 A}{\varepsilon_D} u_t V_t\Big)\frac{dV_t}{dt} = -\sigma_p \varepsilon_D A \frac{V_t}{\varepsilon_D} \\ &\Big(M_b + \rho_0 L_0 A - \frac{\rho_0 A}{\varepsilon_D} u_t\Big) a_t = -\sigma_p A \end{aligned} \tag{2.18}$$

and

$$a_t = \frac{\sigma_p \varepsilon_D}{\rho_0 u_t - m\varepsilon_D - \rho_0 L_0 \varepsilon_D} \qquad m = \frac{M_b}{A} \tag{2.19}$$

Taking parameter symbols of I, J and K into account, Eq. $(2.19)_1$ is equivalently expressed as

$$a = \frac{I}{Ju - K} \tag{2.20}$$

and

$$I = \sigma_p \varepsilon_D \qquad J = \rho_0 \qquad K = m\varepsilon_D + \rho_0 L_0 \varepsilon_D \tag{2.21}$$

Based on acceleration-displacement Eqs. (2.20) and (2.21), one can conclude that acceleration of the protected product is related with density, compact strain, and platform stress of the cushioning material. The acceleration-displacement equation of the protected product can be calculated by the parameters of I, J and K. I is the combination of the platform stress and compact strain, which is the maximum energy absorption per unit volume of the cushioning material. J is density of the cushioning material. K depens on the compact strain, density, section area, original length of the cushioning material, and the protected product mass.

3. Numerical validation of theoretical model

To verify the theoretical model in Eq. (2.20), three polymer foam cushioning materials (EPS, FPUF, RPUF) are selected for the packaging container. The geometric dimensions of the packaging container are shown in Fig. 3. The container shell is made of aluminium. The inner and outer diameters of the shell are 72 mm and 78 mm, respectively. The protected product is a steel cylinder. The diameter and height are 72 mm and 78 mm. The two cushioning layers are with

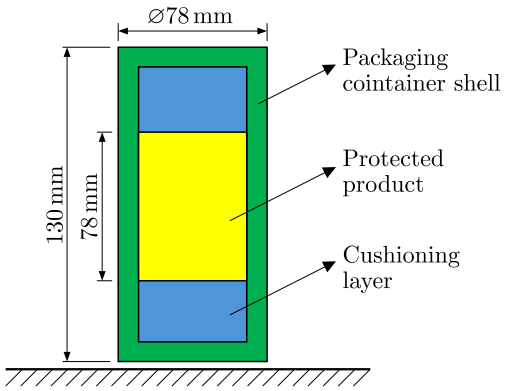

Fig. 3. Geometric diagram of packaging container

Table 1. Geometric paraneters of the packaging container

Parameter	Diameter [mm]	Height [mm]	Thickness [mm]
Outer shell	78	130	3
Protected product	72	78	–
Cushioning layer	72	20	–

the same size. The diameter and height of the cushioning layer are 72 mm and 20 mm. Detailed geometrical information is given in Table 1.

Taking density of the protected product as 7810 kg/m^3, then area density is 609.18 kg/m^2. The densities, equivalent platform stresses and compaction strains of EPS, FPUF and RPUF are cited from the references of Zhang *et al.* (2022, 2023). The initial impact velocity of the packaging container is 9.8 m/s. The parameters I, J, K for EPS, FPUF, and RPUF at the strain rate of 100/s are calculated by Eqs. (2.21), see Table 2.

Table 2. Cushioning material mechanical properties and design parameters

Material	Density [kg/m^3]	Platform stress [MPa]	Compaction strain	I	J	K
EPS-100/s	43.5	0.566	0.660	373390	43.5	402.633
FPUF-100/s	77.8	0.045	0.560	25431	77.8	342.012
RPUF-100/s	125.6	2.417	0.630	1522518	125.6	385.366

The finite element model of the packaging container is shown in Fig. 4. The material of the protected product and the target plate is steel. The container shell is made of aluminium. The mechanical properties of packaging container materials are shown in Table 3. An elastic-plastic constitutive model is adopted to describe mechanical behaviour of steel and aluminium. A crushable foam model is adopted to describe mechanical behaviour of EPS and RPUF. The mechanical behaviour of FPUF is described by the hyperfoam constitutive model. The compressive stress-strain curves of EPS, FPUF, RPUF at the strain rate of 100/s are shown in Fig. 5.

Figure 6 shows von Mises stress and equivalent plastic strain of the packaging container when the protected product velocity is 0. The packaging containers of FPUF, RPUF exhibit the highest and lowest equivalent plastic strain, respectively. It indicates that FPUF was a lower energy absorption, and energy absorption capacity of RPUF is stronger. The whole cushioning

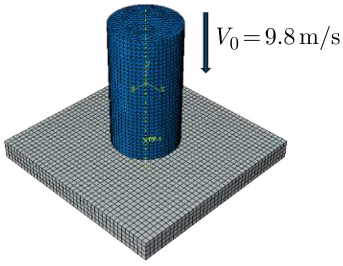

Fig. 4. Finite element model of the packaging container

Table 3. Material properties of the packaging container

Material	Density [kg/m^3]	Elastic modulus [MPa]	Poisson's ratio	Yield stress [MPa]
Aluminium	2700	69000	0.30	290
Steel	7810	212000	0.30	460
EPS-100/s	43.5	9.29	0.01	–
FPUF-100/s	77.8	0.91	0.01	–
RPUF-100/s	125.6	45.30	0.01	–

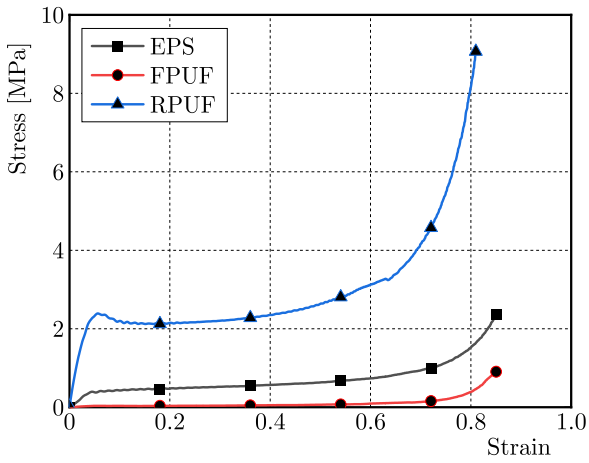

Fig. 5. Compressive stress-strain curves of cushioning materials

layer of FPUF is compacted, which results in that the kinetic energy of the protected product can not be absorbed fully by the cushioning material in the impact process. The cushioning material EPS has with a moderate energy absorption capacity. The numerical results show partial compaction of the EPS cushioning layer. In contrast, RPUF has a higher platform stress, which induces the highest energy absorption in the impact process.

The plastic platform stress is taken as constant in the deformation process in Eq. (2.20). The theoretical expression is only feasible in the platform stress stage, namely the protected product displacement is less than $l_0\varepsilon_D$. The expression is not suitable in the compaction stage. Figure 7 is the displacement-time curve comparison of the protected product by theoretical calculation and numerical simulation, respectively. It shows that the cushioning layers of EPS and FPUF are fully compacted in the drop impact process. The results of theoretical analysis and numerical simulation are consistent before the compaction stage, which verifies reliability of the theoretical analysis.

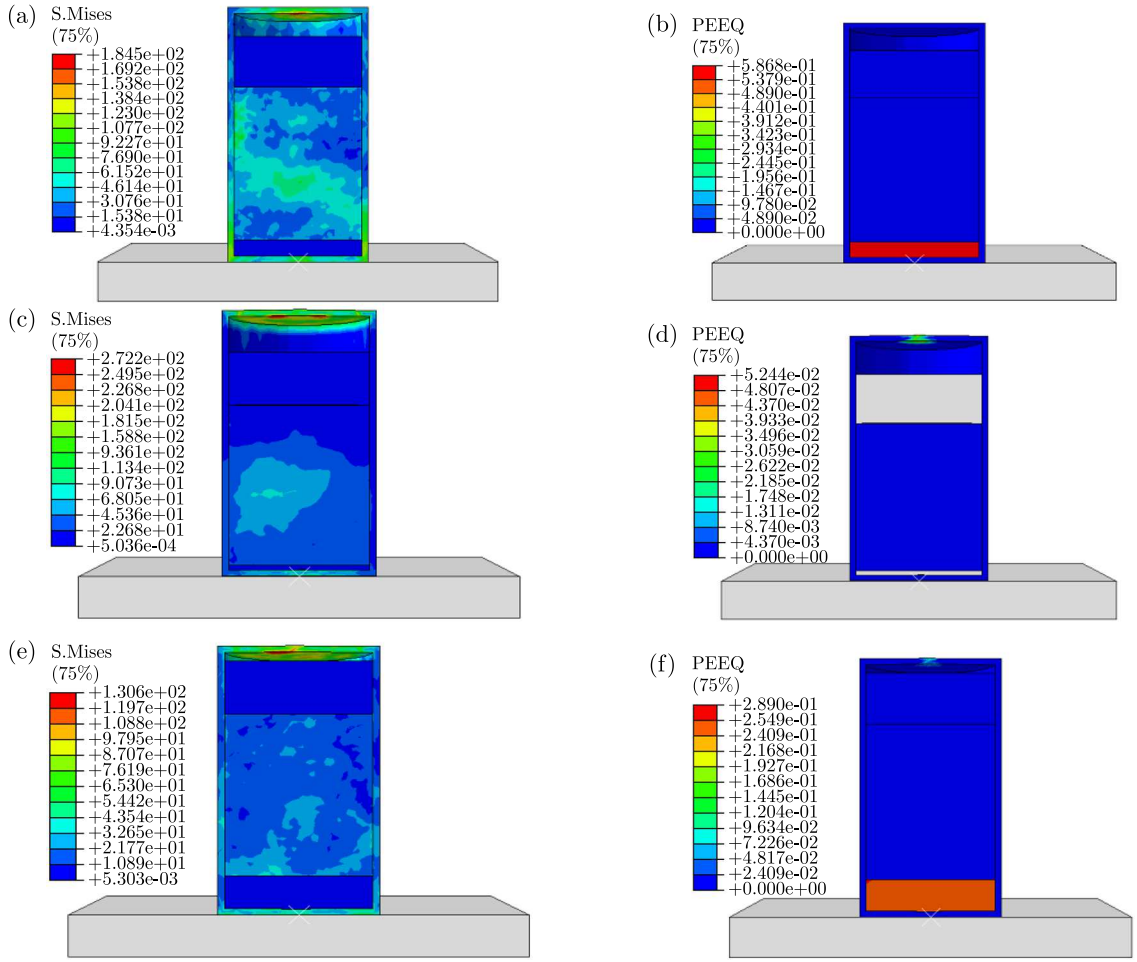

Fig. 6. Von Mises stress and equivalent strain of the packaging container: (a) EPS stress, (b) EPS plastic strain, (c) FPUF stress, (d) FPUF plastic strain, (e) RPUF stress, (f) RPUF plastic strain

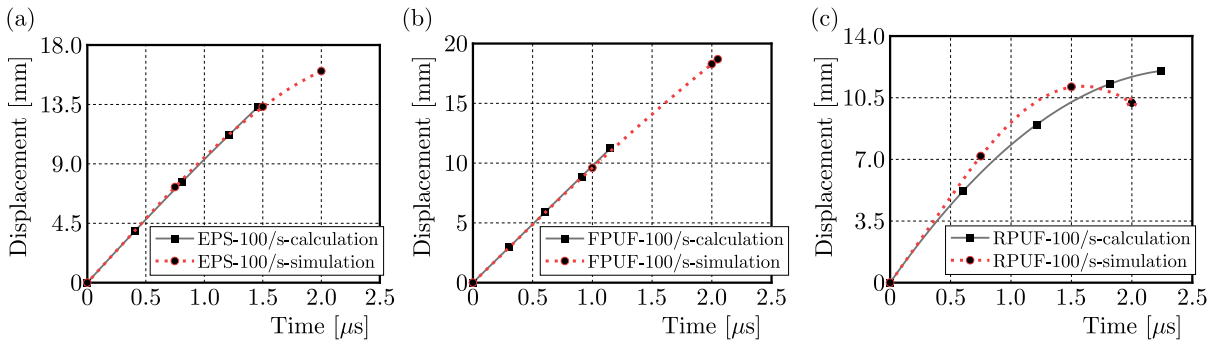

Fig. 7. Displacement-time curve comparison of the protected product by theoretical analysis and simulation: (a) EPS, (b) FPUF, (c) RPUF

For the RPUF cushioning material, the theoretical result is not consistent well with that of simulation in the large deformation stage. An assumption of the cushioning material with constant platform stress until reaching the densification stage is made. It means that elastic energy absorption is small and can be ignored comparing to the plastic deformation energy. Being different from EPS and FPUF, the elastic energy absorption of RPUF is relatively larger. It induces a discrepancy between the theoretical analysis and numerical simulation, which is increases with growth of the deformation.

4. Influence of the strain rate on the impact protection effectiveness under the lateral constraint condition

Polymer foam materials are usually sensitive to the strain rate (Hwang *et al.*, 2020; Tateyama *et al.*, 2016). In order to investigate the influence of the strain rate on the impact protection effectiveness of the cushioning material under the lateral constraint condition, packaging container (see Fig. 3) with initial impact velocity 9.8 m/s is analysed. During the packaging container impact process, the strain rate of the cushion layer is taken as constant. The mechanical properties of cushioning materials under different strain rate conditions are substituted into the theoretical model. The effect of strain rate on the impact protection effectiveness of cushioning materials under the lateral constraint condition is analysed. The stresses and compaction strains of EPS, FPUF and RPUF at strain rates of 1/s, 10/s, and 100/s are cited from the preliminary work (Zhang *et al.*, 2022, 2023). The parameters I, J, K of the three cushioning materials are calculated by Eqs. (2.21), see Table 4.

Table 4. Cushioning material design parameters at different strain rate conditions

Material	Density [kg/m^3]	Platform stress [MPa]	Compaction strain	I	J	K
EPS-1/s	43.5	0.415	0.660	273902	43.5	402.633
EPS-10/s	43.5	0.466	0.660	307291	43.5	402.633
EPS-100/s	43.5	0.566	0.660	373390	43.5	402.633
FPUF-1/s	77.8	0.025	0.560	13744	77.8	342.012
FPUF-10/s	77.8	0.034	0.560	19125	77.8	342.012
FPUF-100/s	77.8	0.045	0.560	25431	77.8	342.012
RPUF-1/s	125.6	2.029	0.630	1278195	125.6	385.366
RPUF-10/s	125.6	2.256	0.630	1421101	125.6	385.366
RPUF100/s	125.6	2.47	0.630	1522517	125.6	385.366

The energy absorbing capacity of the cushioning material and the maximum acceleration of the protected product are applied to evaluate the impact protection effectiveness of the packaging container. The acceleration of the protected product is equivalent to the stress propagating to the protected product. For the protected product safety, the stress is not allowed to exceed the bearing limit of the product material. A greater energy absorption of the cushioning material induces a lower acceleration of the protected product, which brings a better impact protection of the packaging container.

Figure 8 shows the displacement-time and velocity-time curves of the protected product found by theoretical calculations. The residual velocity of the protected product decreases with the increasing strain rate at the three strain rate conditions. It indicates that a high strain rate enhances the energy absorbtion of the three cushioning materials under lateral constraint conditions. Comparing with EPS and FPUF, the velocity of the protected products in RPUF containers is lower. It means that the EPS and FPUF cushioning layers are fully compacted, and the RPUF cushioning layer is partly compacted in the impact condition.

Figure 9 shows the maximum acceleration of the protected product during the packaging container impacting process. It is evident that a higher strain rate results in a higher acceleration of the protected product. The cushioning layer exhibits greater energy absorption at higher strain rate conditions. However, a higher strain rate loading brings leads to a higher stress of the protected product. The energy absorption and allowable stress should be considered designing in the packaging container.

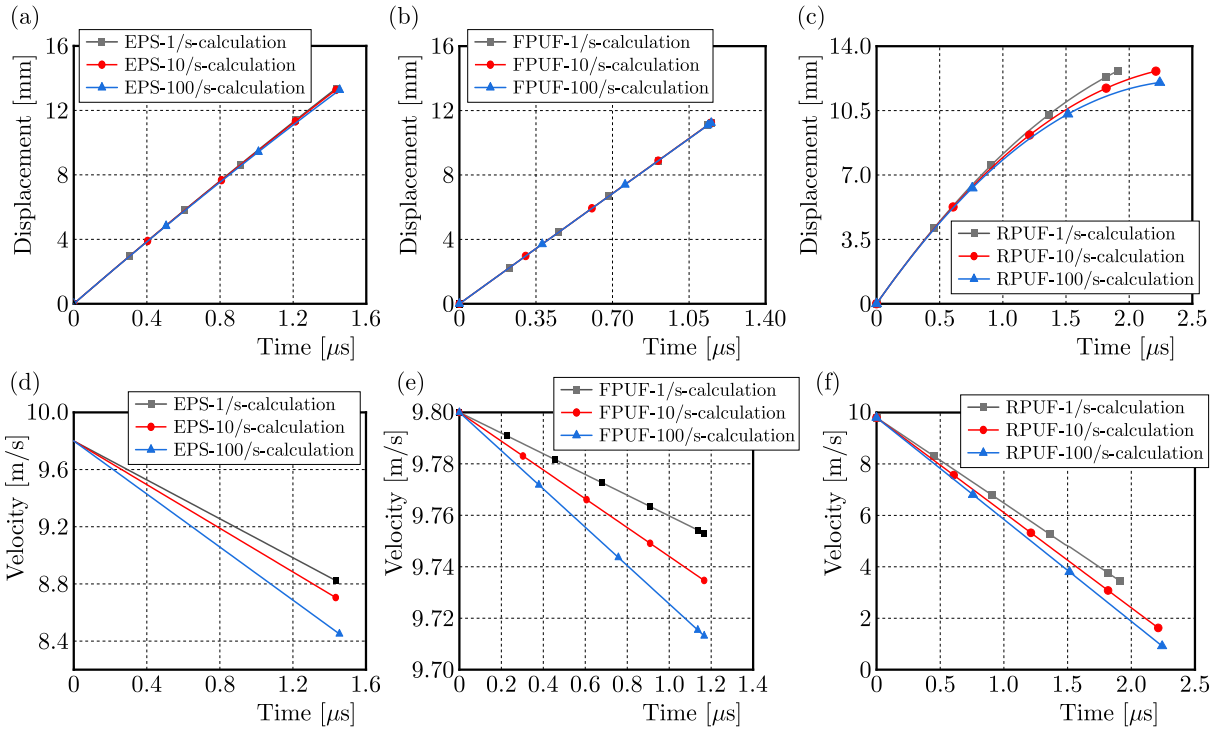

Fig. 8. Theoretical results for the packaging container: (a) EPS displacement, (b) FPUF displacement, (c) RPUF displacement, (d) EPS velocity, (e) FPUF velocity, (f) RPUF velocity

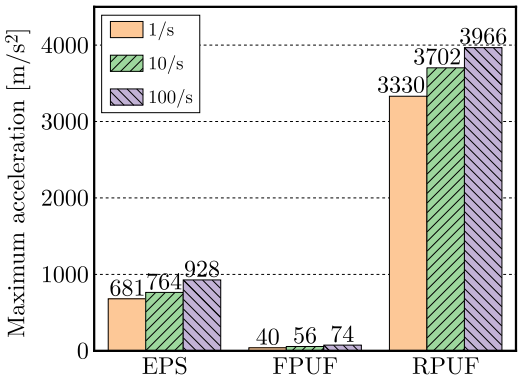

Fig. 9. Maximum acceleration of the protected product

5. Finding the cushioning material thickness in the packaging container

Once the cushioning material in the packaging container is compressed into the densification state, the internal space of the cushioning material is filled, and the stress increases sharply. For a high performance cushioning material, the platform stress should be stable under a large deformation condition. According to Eq. (2.20), the acceleration of the protected product in the packaging container increases with growing displacement. For ideal cushioning design, the cushioning material should be with little compaction rather than full compaction when the protected product reaches the maximum displacement. The maximum displacement is given as

$$u_{max} = \varepsilon_D L_0 \tag{5.1}$$

Taking Eq. (2.20) and Eq. (5.1) into account, the maximum acceleration a_{max} of the protected product is expressed as

$$a_{max} = -\frac{I}{K - Ju_{max}} = -\frac{\sigma_p \varepsilon_D}{m\varepsilon_D + \rho_0 L_0 \varepsilon_D - \rho_0 \varepsilon_D L_0} = -\frac{A\sigma_p}{m_b} \tag{5.2}$$

When the maximum acceleration is less than the allowance value of the protected product, the thickness of the cushioning material is given as follows

$$T = C_{min}\frac{Hg}{a_{max}} = C_{min}\frac{Hgm_b}{A\sigma_p} \tag{5.3}$$

C_{min} represents the minimum cushioning coefficient, H is the allowance drop height for the packaging container, and g is the gravity acceleration. Table 5 shows the minimum cushioning coefficients of EPS, FPUF and RPUF at strain rates of 1/s, 10/s and 100/s obtained from experimental tests (Zhang *et al.*, 2022, 2023). Based on the protected product (see Fig. 3, the mass is 2.45 kg and the section area is 4069 mm^2) and the platform stresses in polymer foam materials (Table 3), the minimum cushioning coefficients of polymer foam materials are presented in Table 5. The theoretical minimum thickness of the cushioning materials under the impact condition of 9.8 m/s is listed in Table 6. It is contributed to optimize the cushioning layer in the packaging container and to enhance the impact protection performance.

Table 5. Minimum cushioning coefficient of the cushioning material

Strain rate	1/s	10/s	100/s
Minimum cushioning coefficient for EPS	2.323	2.429	2.369
Minimum cushioning coefficient for FPUF	3.324	3.239	3.056
Minimum cushioning coefficient for RPUF	2.380	2.369	2.215

Table 6. Theoretical design thickness of the cushioning material

Strain rate	1/s	10/s	100/s
Thickness for EPS [mm]	167	156	125
Thickness for FPUF [mm]	4042	2831	2009
Thickness for RPUF [mm]	35	31	27

6. Conclusion

- Based on the stress wave theory and energy conservation law, a theoretical model for packaging containers during the drop impact is proposed. The acceleration-displacement equation of the protected product is derived. It indicates that the product acceleration is affected by the cushioning material density, compaction strain, and platform stress.
- The displacement-time variation of the protected product in packaging containers filled with cushioning materials EPS, FPUF and RPUF, respectively, is obtained by theoretical analysis and numerical simulations. The two approaches achieve consistent results.
- Combining the acceleration-displacement equation of the protected product and the mechanical properties of EPS, FPUF, RPUF under different strain rates, the influence of the strain rate on the impact protection effectiveness of cushioning materials under the lateral constraint condition is analysed. It shows that a high strain rate brings container's improvement of the ultimate bearing capacity of the container, but induces higher stress in the protected product.

- The formula for thickness determination of the cushioning material is derived. The optimum thickness of the cushioning material is related with impact velocity, bearing area, and protected product mass.

Acknowledgement

The authors gratefully acknowledge the funding by National Natural Science Foundation of China under contract No.12172344.

References

1. An X., Shi D., 2022, An innovation active set strategy reliability optimization method for cushioning design based on dynamic stress-strain curve, *Packaging Technology and Science*, **35**, 2, 153-162
2. Baertsch F., Ameli A., Mayer T., 2021, Finite-element modeling and optimization of 3D-printed auxetic reentrant structures with stiffness gradient under low-velocity impact, *Journal of Engineering Mechanics*, **147**, 7, DOI: 10.1061/(ASCE)EM.1943-7889.0001923
3. Baroutaji A., Gilchrist M.D., Olabi A.G., 2016, Quasi-static, impact and energy absorption of internally nested tubes subjected to lateral loading, *Thin-Walled Structures*, **98**, Part B, 337-350
4. Chang J., Gong X., Sun Z., 2017, Analysis of mechanical properties of glass packaging, advanced graphic communications and media technologies, [In:] *Advanced Graphic Communications and Media Technologies, PPMT 2016, Lecture Notes in Electrical Engineering*, Zhao P., Ouyang Y., Xu M., Yang L., Ouyang Y. (Eds.), **417**, Springer, Singapore, 635-641
5. Estrada Q., Szwedowicz D., Majewski T., Oliver M., Cortes C,. Castro F., 2017, Effect of discontinuity size on the energy absorption of structural steel beam profiles, *Mechanics of Advanced Materials and Structures*, **24**, 1, 88-94
6. Guo Y., Han X., Wang X., Fu Y., Xia R., 2021, Static cushioning energy absorption of paper composite sandwich structures with corrugation and honeycomb cores, *Journal of Sandwich Structures and Materials*, **23**, 4, 1347-1365
7. Gupta N., 2007, A functionally graded syntactic foam material for high energy absorption under compression, *Materials Letters*, **61**, 4-5, 979-982
8. Hussain N.N., Regalla S.P., Rao Y.V. D., Dirgantara T., Gunawan L., Jusuf A., 2021, Drop-weight impact testing for the study of energy absorption in automobile crash boxes made of composite material, *Proceedings of the Institution of Mechanical Engineers, Part L: Journal of Materials: Design and Applications*, **235**, 1, 114-130
9. Hwang B.K., Kim S.K., Kim J.H., Kim J.D., Lee J.M., 2020, Dynamic compressive behavior of rigid polyurethane foam with various densities under different temperatures, *International Journal of Mechanical Sciences*, **180**, 105657
10. Kader M.A., Islam M.A., Hazell P.J., Escobedo J.P., Saadatfar M., *et al.*, 2016, Modelling and characterization of cell collapse in aluminium foams during dynamic loading, *International Journal of Impact Engineering*, **96**, 78-88
11. Karagiozova D., 2011, Velocity attenuation and force transfer by a single- and double-layer claddings made of foam materials, *International Journal of Protective Structures*, **2**, 4, 417-437
12. Koohbor B., Kidane A., 2016, Design optimization of continuously and discretely graded foam materials for efficient energy absorption, *Materials and Design*, **102**, 151-161
13. Luong V.D., Bonnin A.S., Abbès F., Nolot J.B., Erre D., Abbès B., 2021, Finite element and experimental investigation on the effect of repetitive shock in corrugated cardboard packaging, *Journal of Applied and Computational Mechanics*, **7**, 2, 820-830
14. Lye S.W., Lee S.G., Chew B.H., 2004, Virtual design and testing of protective packaging buffers, *Computers in Industry*, **54**, 2, 209-221

15. Meng Y., Lin Y., Zhang Y., Li X., 2020, Study on the dynamic response of combined honeycomb structure under blast loading, *Thin-Walled Structures*, **157**, 107082

16. Pan Y., Yu K., 2022, Simulation analysis of packaging box for free fall airdrop, *2022 International Conference on Applied Physics and Computing (ICAPC)*, Ottawa, Canada, 374-378

17. Reid S.R., Peng C., 1997, Dynamic uniaxial crushing of wood, *International Journal of Impact Engineering*, **19**, 5-6, 531-570

18. Sek M.A., Rouillard V., 2006, Behaviour of multi-layered corrugated paperboard cushioning systems under impact loads, *Applied Mechanics and Materials*, **3-4**, 383-390

19. Tateyama K., Yamada H., Ogasawara N., 2016, Effect of strain rate on compressive properties of foamed polyethylene film, *Polymer Testing*, **52**, 54-62

20. Zeng H.B., Pattofatto S., Zhao H., Girard Y., Fascio V., 2010, Impact behaviour of hollow sphere agglomerates with density gradient, *International Journal of Mechanical Sciences*, **52**, 5, 680-688

21. Zhang G.Q., Huang J., Lin H.B., 2011, Dynamical simulation about buffer packaging of computer, *Applied Mechanics and Materials*, **55-57**, 1711-1724

22. Zhang Z., Zhong W., Chen J., Luo, J., 2022, Compressive properties and energy absorption of rigid polyurethane foam, *Journal of Physics: Conference Series*, **2368**, 012013

23. Zhang Z., Zhong W., Chen J., Luo J., Li J., Huang X., 2023, Influence of strain rate and temperature on compressive properties and energy absorption efficiency of expanded polystyrene and flexible polyurethane foam, *Mechanika*, **29**, 6, 445-453

Manuscript received July 7, 2024; accepted for publication October 11, 2024